Electronic Supplementary Information

Spin-glass Behavior of a Hierarchically-Organized, Hybrid Microporous Material, Based on an Extended Framework of Octanuclear Iron-Oxo Units

Xin-Yi Cao,[†] Jeremiah W. Hubbard,[§] Jennifer Guerrero-Medina,[§] Arturo J. Hernández-Maldonado,[§] Logesh Mathivathanan,[†] Carlos Rinaldi,[§,#,*] Yiannis Sanakis,[‡,*] and Raphael G. Raptis[†,*]

[†] Department of Chemistry and Institute for Functional Nanomaterials, University of Puerto Rico, San Juan, PR 00936-8377. Present address: Department of Chemistry and Biochemistry, Florida International University, Miami, FL 33199.

[‡] Institute of Materials Science, NCSR "Demokritos", 15310 Aghia Paraskevi, Athens, Greece.

[§] Department of Chemical Engineering, University of Puerto Rico-Mayagüez Campus, Mayagüez, PR 00681-9000.

[#] Present address: J. Crayton Pruitt Family Department of Biomedical Engineering and Department of Chemical Engineering, University of Florida, Gainesville, FL 32611.

Fax: (305) 348-3772

E-mail: rraptis@fiu.edu (R. G. R.); sanakis@ims.demokritos.gr (Y. S.); carlos.rinaldi@bme.ufl.edu (C. R.)

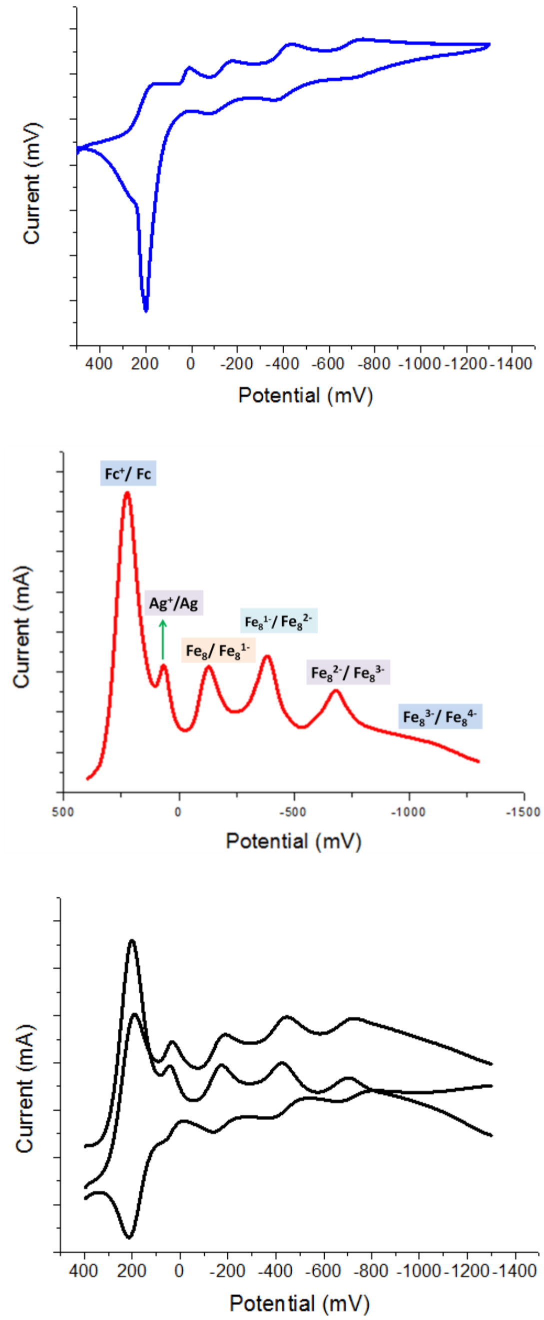

Figure S1. CV (top), DPV (middle) and OSWV (bottom) of intermediate cluster ion $[Fe_8(\mu_4\text{-}O)_4(\mu\text{-}pz)_{12}(CH_3CN)_4]^{4+}$ in 0.5 M $Bu_4N{\cdot}PF_6$ of CH_2Cl_2/CH_3CN solution using a non-aqueous $Ag/AgNO_3$ reference electrode, Pt auxiliary electrode, and Pt working electrode.

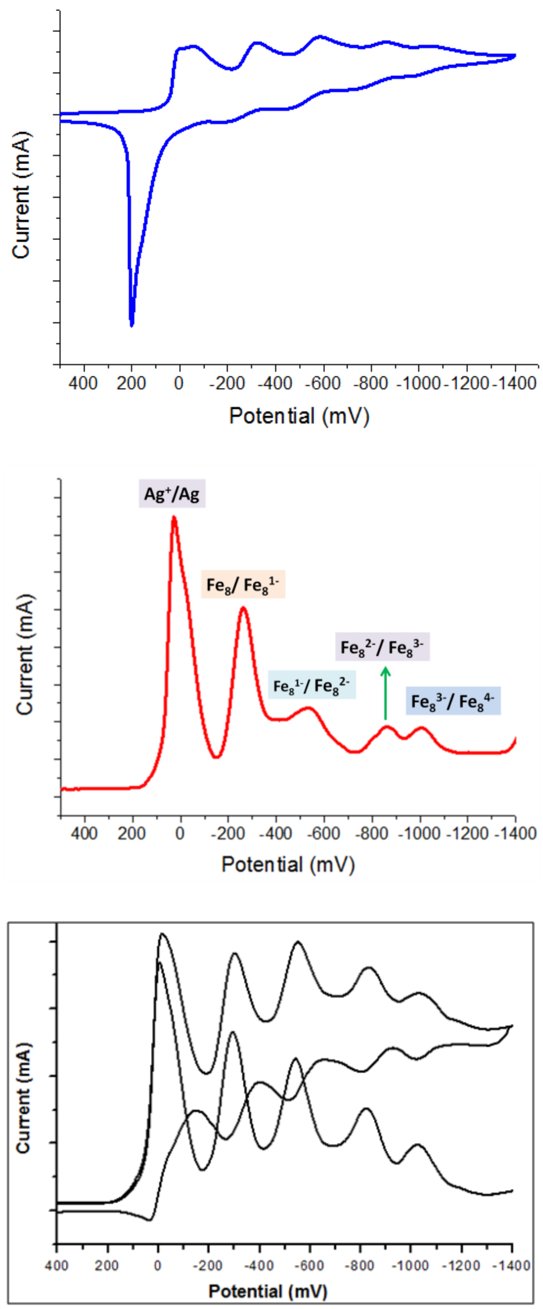

Figure S2. CV (top), DPV (middle) and OSWV (bottom) of intermediate cluster ion $[Fe_8(\mu_4\text{-}O)_4(\mu\text{-}4\text{-}Me\text{-}pz)_{12}(CH_3CN)_4]^{4+}$ in 0.5 M $Bu_4N{\cdot}PF_6$ of CH_2Cl_2/CH_3CN solution using a non-aqueous $Ag/AgNO_3$ reference electrode, Pt auxiliary electrode, and Pt working electrode.

Table S3. Cyclic voltammetric data for intermediate clusters and their corresponding parent clusters in CH_2Cl_2/CH_3CN at 298 K.

	Potential, V			
	$E_{1/2}$ (1)	$E_{1/2}$ (2)	$E_{1/2}$ (3)	$E_{1/2}$ (4)
$[Fe_8(\mu_4\text{-}O)_4(\mu\text{-pz})_{12}(CH_3CN)_4]^{4+}$	-0.36	-0.61	-0.92	---
$[Fe_8(\mu_4\text{-}O)_4(\mu\text{-pz})_{12}Cl_4]$	-0.43[a]	-0.78[a]	-0.107[a]	-1.38[a]
$[Fe_8(\mu_4\text{-}O)_4(\mu\text{-4-Me-pz})_{12}(CH_3CN)_4]^{4+}$	-0.49	-0.77	-1.09	-1.24
$[Fe_8(\mu_4\text{-}O)_4(\mu\text{-4-Me-pz})_{12}Cl_4]$	-0.58[a]	-0.91[a]	-1.20[a]	-1.55[a]

[a] Data from ref. 9b.

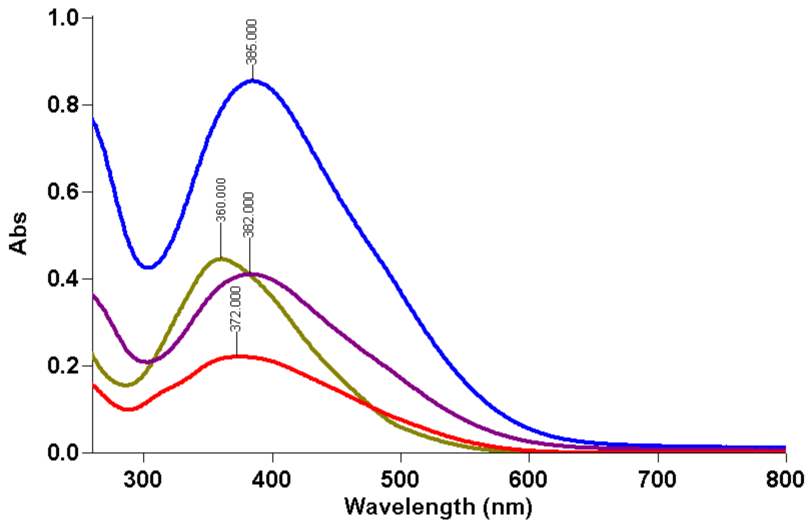

Figure S4. UV-Vis-NIR spectroscopies of intermediate clusters and their corresponding parent clusters in CH_2Cl_2/CH_3CN at 298 K with $[Fe_8(\mu_4\text{-}O)_4(\mu\text{-pz})_{12}(CH_3CN)_4]^{4+}$ (λ_{max} = 382 nm), $[Fe_8(\mu_4\text{-}O)_4(\mu\text{-pz})_{12}Cl_4]$ (λ_{max} = 360 nm), $[Fe_8(\mu_4\text{-}O)_4(\mu\text{-4-Me-pz})_{12}(CH_3CN)_4]^{4+}$ (λ_{max} = 385 nm), and $[Fe_8(\mu_4\text{-}O)_4(\mu\text{-4-Me-pz})_{12}Cl_4]$ (λ_{max} = 372 nm).

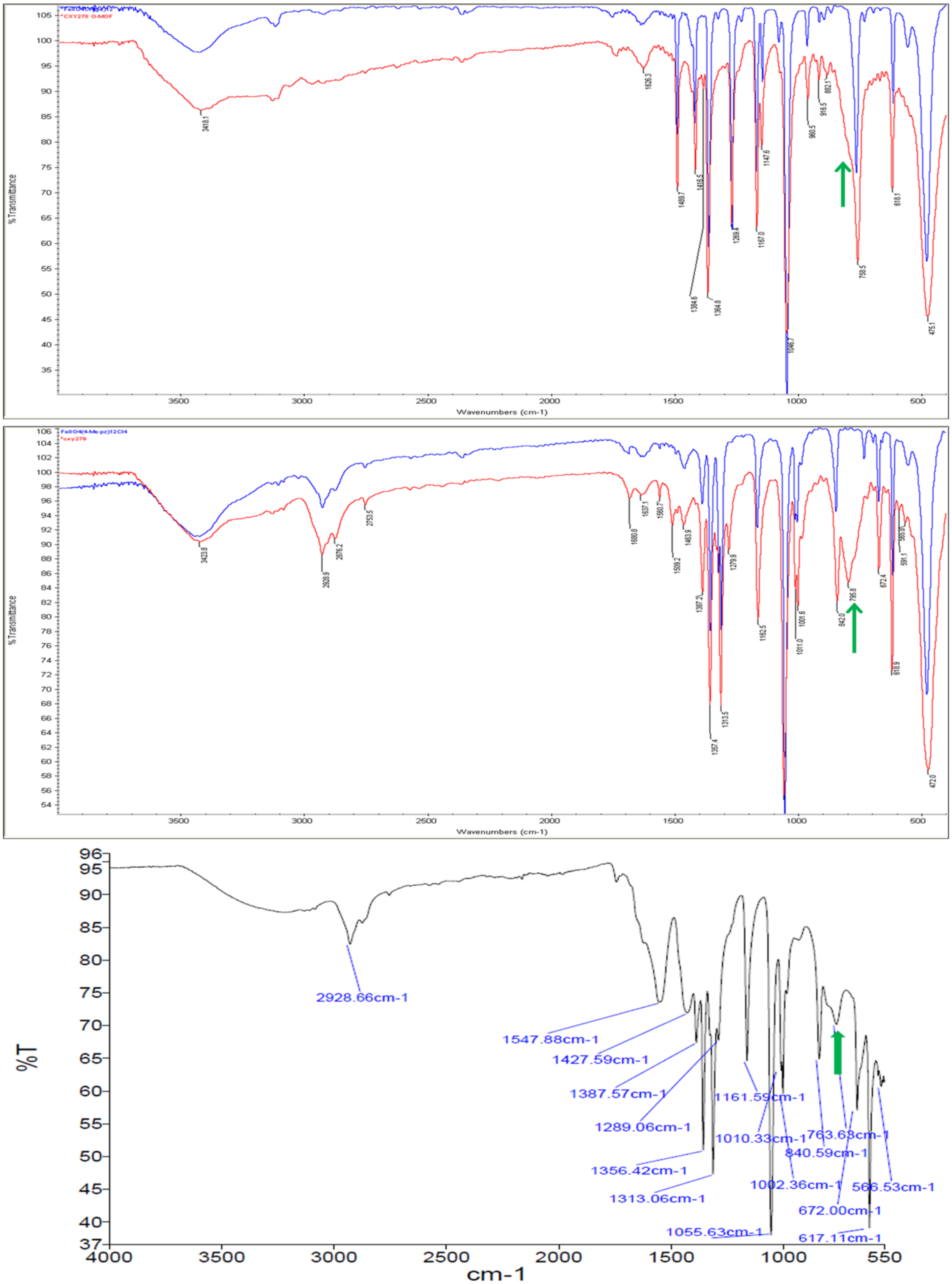

Figure S5. IR spectra of KBR pellets of complexes **1** (upper, red) and **2** (middle, red) and their corresponding parent clusters (blue) and powder sample of ^{18}O-labelled **2** (lower).

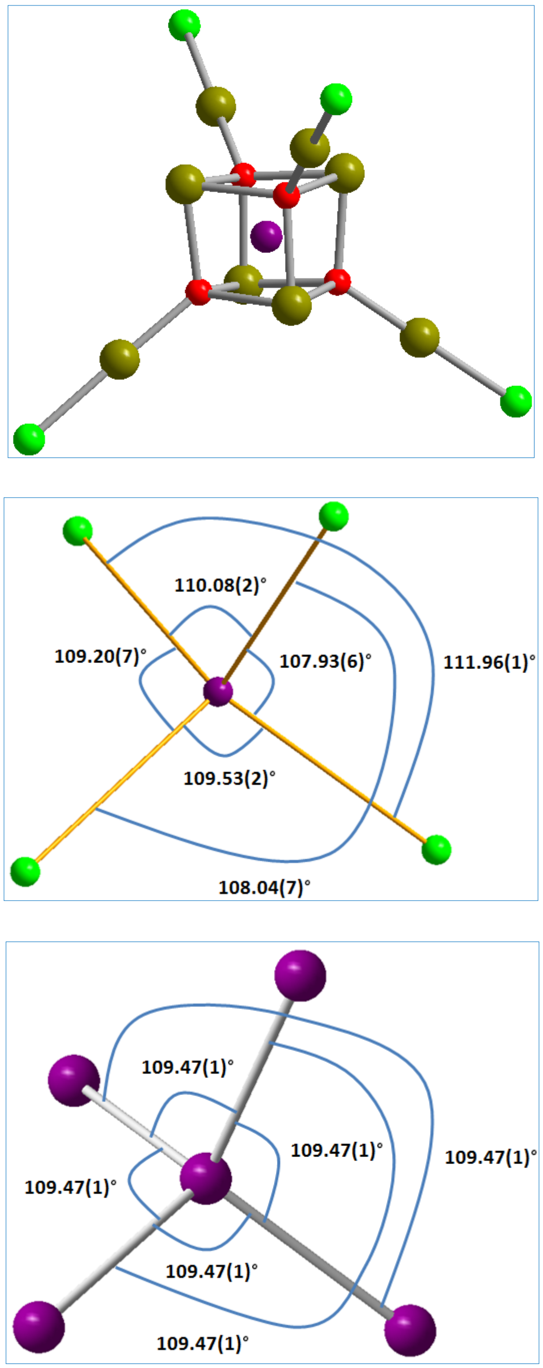

Figure S6. Top figure shows a tetrahedral motif of Fe_8-cluster with an inserted imaginery atom in the center of the cubane; middle is the simplified 4-connected unit of Fe_8-cluster with angle parameters; bottom is the 4-connected unit in diamond network of crystalline cubic silicon.

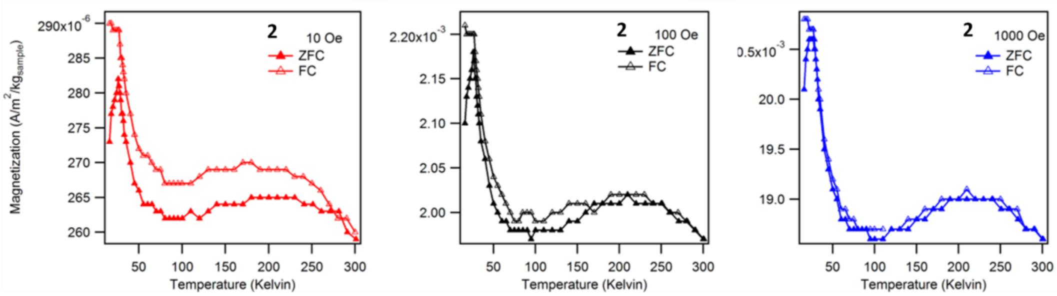

Figure S7. ZFC/FC measurements at various applied magnetic fields for sample **2**. The sample displays a peak in the ZFC curve at ~30 K.

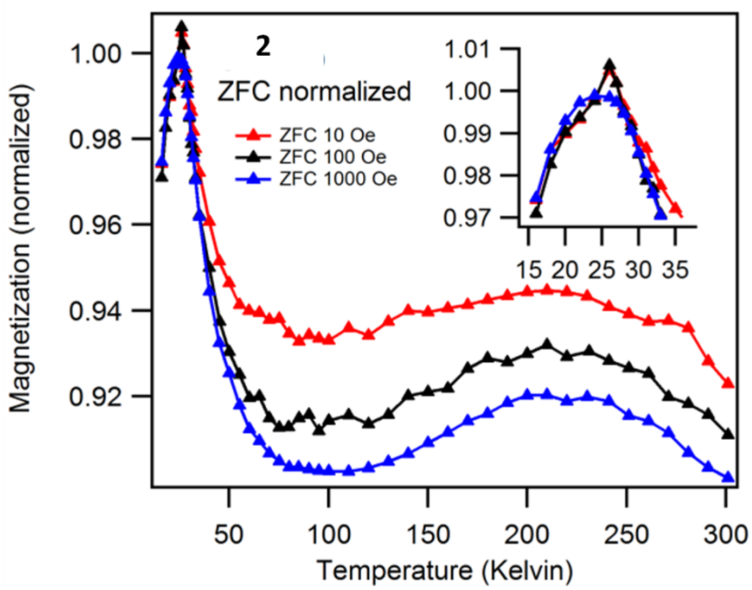

Figure S8. Zero field cooled (ZFC) measurements as a function of field and normalized with respect to peak height for sample **2**. The curves display a peak that is at ~30 K for the low fields and shift slightly to lower temperatures as the field increases (insert).

The field-dependent magnetization, M(H), was measured at selected temperatures (15, 50 and 298.15 K) between ±7 Tesla after cooling in zero field. Hysteresis with weak coercive behavior is observed for **1** and **2** with comparable coercive fields (Hc) of 4 and 2 Oe, respectively. **Fig. S9** shows the equilibrium magnetization measurements at selected temperatures for compound **1**. The magnetic behavior varies with temperature. The insert shows the hysteresis at 15 K. Remanence of 7.31×10^{-3} Am^2/kg_{sample} (emu/g) and coercivity of -10181 A/m were determined for compound **1** at 15 K. **Fig. S10** illustrates the equilibrium magnetization measurements at selected temperatures for compound **2** and the insert shows the hysteresis at 15 K. This sample shows similar magnetic behavior at the measured temperatures, with a remanence of 2.08×10^{-3} Am^2/kg_{sample} (emu/g) and coercivity of -6813 A/m at 15 K.

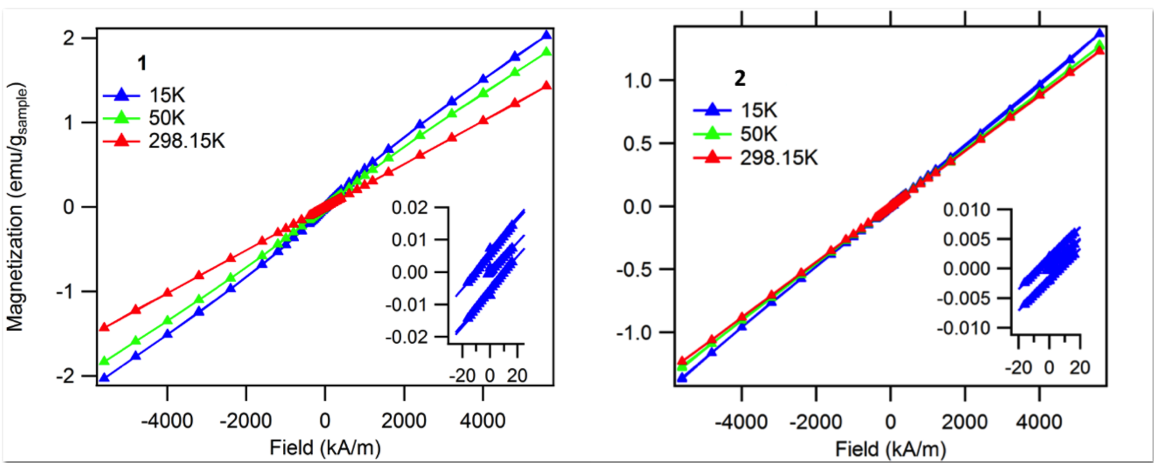

Fig. S9. Equilibrium magnetization measurements at selected temperatures for complex **1** (left) and **2** (right). The insert shows the hysteresis at 15 K.

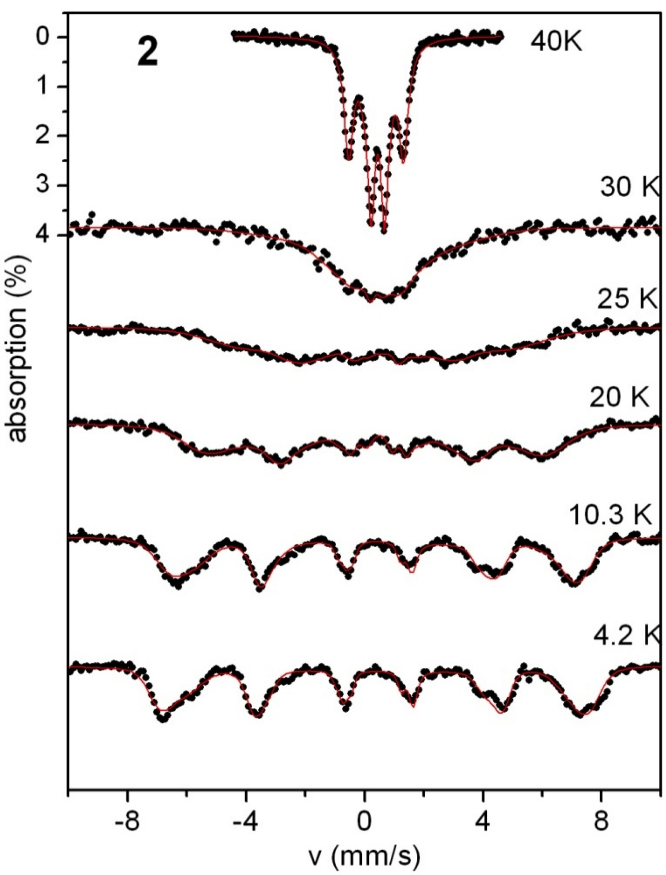

Figure S10. Temperature dependence of Mössbauer spectrum of **2**. Red lines are simulations.